

Physics of compact stellarators*

S. P. Hirshman,[†] D. A. Spong, J. C. Whitson, B. Nelson, D. B. Batchelor, J. F. Lyon,
and R. Sanchez

Oak Ridge National Laboratory, Oak Ridge, Tennessee 37831-8071

A. Brooks, G. Y.-Fu, R. J. Goldston, L.-P. Ku, D. A. Monticello, H. Mynick, G. H. Neilson,
N. Pomphrey, M. Redi, W. Reiersen, A. H. Reiman, J. Schmidt, R. White, and
M. C. Zarnstorff

Princeton Plasma Physics Laboratory, Princeton, New Jersey 08543

W. H. Miner, Jr. and P. M. Valanju

University of Texas at Austin, Austin, Texas 78712-1081

A. Boozer

Department of Applied Physics, Columbia University, New York, New York 10027

(Received 12 November 1998; accepted 27 January 1999)

Recent progress in the theoretical understanding and design of compact stellarators is described. Hybrid devices, which depart from canonical stellarators by deriving benefits from the bootstrap current which flows at finite beta, comprise a class of low aspect ratio $A < 4$ stellarators. They possess external kink stability (at moderate beta) in the absence of a conducting wall, possible immunity to disruptions through external control of the transform and magnetic shear, and they achieve volume-averaged ballooning beta limits (4%–6%) similar to those in tokamaks. In addition, bootstrap currents can reduce the effects of magnetic islands (self-healing effect) and lead to simpler stellarator coils by reducing the required external transform. Powerful physics and coil optimization codes have been developed and integrated to design experiments aimed at exploring compact stellarators. The physics basis for designing the national compact stellarator will be discussed.

[S1070-664X(99)95405-8]

I. INTRODUCTION

Interest in compact stellarators, for which the average aspect ratio $A \equiv R/a < 4$, derives from both the desire to design a fusion reactor of economical size and to combine the favorable features of tokamaks (good confinement, high β) and stellarators (low recirculating power, lack of disruptions). Here, R is the mean major radius, and a is the plasma (minor) radius. Existing stellarators have $A > 5$ [Compact Helical System¹ (CHS) and Compact Auburn Torsatron² (CAT)]. Transport optimized stellarators under construction [Wendelstein-7X (W7X),³ $A = 11$] and nearing completion [Helically Symmetric Experiment⁴ (HSX), $A = 8$] are large aspect ratio compared with tokamaks. The research described here focuses on hybrid stellarator configurations with aspect ratios in the range $2 < A < 4$, in which the self-consistent bootstrap current provides some fraction of the rotational transform, ι . These configurations can be tested in moderately sized devices, $R = 1 - 1.5$ m, that are being designed as part of the national compact stellarator program aimed at exploring the physics of compact stellarators.

For compact stellarators to be reactor relevant, the plasma-coil separation Δ must be large enough to accommodate coil shielding and a blanket in a reactor. The minimum reactor size, based on $\Delta \geq 2$ m and scaled from a device with

a gap ratio $A_\Delta \equiv R/\Delta$, would therefore be $R = (2 \text{ m})A_\Delta$. Large A stellarators³ with $A_\Delta > 10$ scale to reactors with $R > 20$ m. The hybrid designs considered here attain $A_\Delta < 7$ (and in some cases, $A_\Delta < 3$) by providing a substantial fraction of the rotational transform through internal (bootstrap) currents. Reducing the magnetic ripple through quasi-axisymmetry allows the coils to be further removed from the plasma. Also, low numbers of field periods N ($N \leq 4$) yield adequate spatial decay lengths for the rippled magnetic field present in nonsymmetric configurations.

The large transport losses of classical stellarators at reactor collisionalities have been overcome in two different ways. Quasi-axisymmetric stellarators⁵ (QAS) achieve tokamak-like neoclassical transport levels by tailoring the spectrum of $|B|$ to be nearly axisymmetric in Boozer flux coordinates. These devices have bootstrap current comparable to a tokamak with the same ι . Unlike a tokamak, QAS can have an ι profile which is modified by external coils to produce positive edge shear, $\iota'/\iota > 0$, where $\iota' = d\iota/d\Phi$ and Φ is the toroidal flux. This imparts kink and neoclassical-tearing stability (magnetic island suppression).⁶ Three-dimensional rippling of the outer surface can also stabilize kink modes in stellarators.⁷ In contrast, quasi-omnigenous stellarators⁸ (QOS) rely on aligning the second adiabatic invariant J^* with magnetic flux surfaces to achieve low transport. QOS can have a transform profile similar to QAS, but with smaller values of the bootstrap current.

The analyses of these configurations necessarily rely on

*Paper J5I1.1 Bull. Am. Phys. Soc. **43**, 1775 (1998).

[†]Invited speaker.

complex, three-dimensional numerical calculations because of the lack of geometric symmetry associated with low A stellarators. The general configurational parameters leading to low A design are discussed in Sec. II. The development of numerical tools for optimizing equilibria, transport and stability properties at low A (and low N), where the analytic expansion techniques based on $A \gg 1$ and $\iota/N \ll 1$ are invalid, is described in Sec. III. In Sec. IV we discuss the low A designs obtained with these computational tools. Issues relating to coils at low A are presented in Sec. V. A QAS is being proposed as a Proof of Principle (PoP) experiment, the National Compact Stellarator Experiment⁹ (NCSX). It attempts to utilize the existing toroidal field (TF) and poloidal field (PF) coils, as well as the vacuum vessel in the Princeton Beta Experiment (PBX-M) facility. This limits the allowable helical excursion of the plasma and leads to a QAS with $A \approx 3.4$. This is larger than some $A \approx 2.2$ designs which have been developed and have similar physics properties. References to both of these compact QAS configurations will appear throughout this paper.

Although low A complicates theoretical analysis, it can assist in reaching certain physics goals. For a fixed ι , magnetic field B , and major radius R , both the ISS95 empirical scaling¹⁰ for the energy confinement time $\tau_E \sim 1/A^{2.21}$ and the neoclassical $\tau_E \sim (1/A^2)f(A)$ (f depends weakly on A) increase strongly with decreasing A . The critical β for ballooning stability in QAS increases with $1/A$ (similar to tokamaks), a dependence opposite to what is usually observed in stellarators.

II. PHYSICS PARAMETERS FOR COMPACT DEVICES

The equilibrium properties which impact the design of a compact stellarator can be summarized in terms of a few dimensionless parameters characterizing the magnetic configuration: the normalized helical pitch $N/A \equiv 1/A_N$, the toroidicity $\epsilon_t = 1/A$, the rotational transform per field period $\iota_N \equiv \iota/N$, the helical excursion $\epsilon_h = a_h/a$ (a_h is the helical displacement), and $\beta = p/(B^2/2\mu_0)$, the ratio of thermal to magnetic energy. These arise naturally from a dimensional analysis of the magnetohydrodynamic (MHD) energy:

$$W = \int \left[\frac{B^2}{2\mu_0} + p \right] dV. \quad (1)$$

The contributions to W from the toroidal field, poloidal field, and helical field energies are in the ratio $A_N:(1 + \kappa^2)\iota_N^2:(1 + \kappa^2)\epsilon_h^2$, where κ is the flux surface elongation. Here, $A_N \sim 1/\epsilon_t$ measures the effects arising from toroidal curvature $1/R$. Self-similar equilibria (for $\epsilon_t < 1$ and $\iota_N < 1$) can be generated by varying the number of field periods while keeping A_N fixed. This was the basis for the original route to low A proposed for the previous compact torsatron studies.¹¹ It also guides the present studies for which $A_N \approx 1$ (compared to $A_N \approx 2$ for HSX and W7X).

Rather than fixing ι_N , we have retained approximately the same total transform, ι , as N varied. This was done to exclude the $\iota = 0.5$ ($q = 2$) resonant surface from the plasma, which experimentally¹² is found to suppress disruptions and fluctuations associated with tearing activity. A minimum av-

erage value of ι (poloidal flux) required for adequate energetic particle confinement can be estimated from angular momentum conservation: $\Delta r/a \sim \sqrt{E}/a\iota \leq 1/3$. Here, E is the particle energy, and Δr is the orbit displacement. (For QAS- and QOS-sized devices, this implies $\iota > 0.3$.) The scaling of $\beta_{eq} \approx \iota^2/A$, anomalous $\tau_E^{\text{ISS95}} \sim \iota^{0.4}$, and neoclassical energy confinement times all favor larger values of ι . Thus, as N was lowered to decrease A , ι_N increased which led to greater helical excursion of the coils (for a fixed percentage of ι to be externally generated). For QAS, the amount of external transform at the peak design β is about 40%–50%. The external transform percentage in QOS exceeds 50% for $\beta < 5\%$.

The number of field periods considered for these designs is in the range $2 \leq N \leq 4$. The lower limit is set by the amount of rotational transform generated from external coils. The upper limit is established, for QAS, by the requirement for good quasi-axisymmetry, which is difficult to maintain as N increases. In QOS, the required helical and “mirror” ripple fields both decay exponentially from the coils with increasing N . This leads to large A_Δ and complex coils unless $N \leq 4$. For both stellarator types, the number of coils N_c per field period is fixed in a narrow range by the magnetic geometry ($\iota_N, |B|$) and the flux surface reconstructability. Thus, larger values of N imply more total coils, which can lead to unrealizable geometric demands at low A , particularly if the coils must be densely packed on the inboard side of the torus.

Magnetic islands of width $w \sim (\sqrt{\delta B^{\psi}/m\iota'})$ form at rational surfaces where $m = n/\iota_N$ (m is the poloidal mode number, n is the toroidal mode number). Here, δB^{ψ} is the radial component of the resonant field. Thus, large values of m (low ι_N) and significant shear at the rational surface both reduce island size. In addition, the presence of a magnetic well ($\int dl/B$ decreasing away from the magnetic axis) can, at low β , reduce the island widths (“self-healing”).¹³ If bootstrap currents j_{bs} proportional to the pressure gradient p' flow in the direction such that $(\iota'/\iota)j_{bs} > 0$, the resulting helical deficit of current can produce additional neoclassical island healing.¹⁴ For these reasons, the stellarators considered here are designed to have magnetic wells over most of their radial profile. This produces a Mercier stable plasma which satisfies the resistive interchange stability criterion. In QAS with substantial bootstrap current, the edge iota should increase to produce neoclassically stabilized islands. Since the bootstrap current in QOS can flow in either direction, the stable iota profile need not be monotonic and is sensitive to the ratio of helical and “bumpy” magnetic field components.

III. OPTIMIZATION METHOD FOR COMPACT STELLARATOR DESIGN

The optimization approach used here is an extension of the method developed by Nührenberg¹⁵ to design the W7X stellarator. This method separates physics from coil optimization and engineering. Rather than using coils to produce plasmas with specific properties, the plasma boundary is instead allowed to deform helically until the physics targets are

attained. Only after such an optimized stellarator is found are the coils then “reverse-engineered” subject to various constraints, such as coil-to-plasma separation Δ , current density and coil curvature, etc. The advantage of this approach is that it allows a wide range of configurations to be explored, since reconstruction of the plasma surfaces using relatively slow field-line following techniques is avoided through the assumption of nested magnetic surfaces. In practice, this procedure may lead to an undesirable set of coils which may not reproduce the optimized physics with the desired accuracy. Further iteration would then be needed between the specification of the plasma boundary and the evaluation of coils.

The physics optimization is represented mathematically as a minimization of χ^2 , which is a sum of squares of the various physics targets.^{15,16} The physics properties are completely determined by the transform and pressure profiles, and the plasma boundary: $\chi^2 = \chi^2[l, p, x_b]$. Here, x_b are the Fourier coefficients of R and Z describing the boundary magnetic flux surface. In practice p and the desired β are chosen a priori, and the current profile is chosen to be approximately consistent with the bootstrap current.

The VMEC code¹⁷ is used to compute the MHD equilibrium needed to evaluate the physics targets for an arbitrary state x_b . The attainment of an optimized state can be hastened by reducing the number of independent variables x_b . The introduction of a spectrally condensed spectrum for x_b allows a meaningful optimization with 10–30 independent variables. Another approach being considered emulates tokamak optimizations for which only a few significant geometric features (aspect ratio, axis shift, elongation, triangularity) are included in x_b . For a stellarator, these parameters vary toroidally within a field period.

The optimization physics properties may be broadly classified into equilibrium, transport, and stability targets. An example of equilibrium targets is the ι -profile. The values of $\iota(0)$, $\iota(1)$, and ι' near the edge are often specified based on physics considerations discussed in Sec. II. The bootstrap current j_{bs} , another equilibrium target, must be consistent with the magnetic field spectrum and the ι and p profiles in the optimized state. Analytic expressions¹⁸ for the bootstrap current in stellarators possess resonances at the rational surfaces, arising from large excursions of toroidally trapped particles in the low collision frequency regime. A resonance-broadening function, which accounts for particle drifts and collisions, has been developed to detune these resonances:

$$\frac{1}{m\iota - n} \rightarrow \text{Re} \left[\frac{1}{m\iota - n + jw} \right]. \quad (2)$$

Here, $w \sim \ln(1/\delta)$ and δ is found from $\delta^2 = \nu_* \ln(1/\delta)$, where $\nu_* < 1$ is the collisionality parameter. A Monte Carlo δf technique¹⁹ has been used to simulate the effects of non-axisymmetric $|B|_{mn}$ components on j_{bs} in a stellarator. The numerical results for a model $|B| = 1 - \epsilon_t \cos \theta + \epsilon_h \cos(M\theta - N\phi)$, shown in Fig. 1, indicate that the detuning function in Eq. (2) gives a good fit for j_{bs} near the resonances. Here, $\theta(\phi)$ is the poloidal (toroidal) angle. Without this broadening term, it was not possible to calculate equilibria with self-consistent bootstrap current.

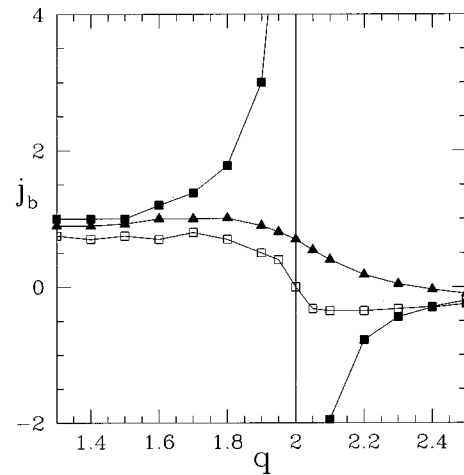


FIG. 1. Bootstrap current j_b for a model magnetic field $|B| = 1 - \epsilon_t \cos \theta + \epsilon_h \cos(M\theta - N\phi)$. Solid squares are the analytic results of Shaing *et al.* (Ref. 18). The resonance is evident at the $q = 1/\iota = 2$ rational surface. The open squares are results from the Monte-Carlo simulation (Ref. 19). Solid triangles result from using the detuning function [Eq. (2)] and show good agreement with the simulation. The parameters used are $\epsilon_h = 0.02s$, $\epsilon_t = 0.22s$, $q = 1 + 4s$, where $s = \Phi/\Phi_w$ and $M = 2$, $N = 1$.

The transport target for QAS is $\partial B / \partial \phi = 0$ (i.e., $|B|_{mn} = 0$ for $n \neq 0$), which is the quasi-axisymmetry condition. Pseudo-symmetry targets have been developed which directly minimize ripple wells in (Boozer) coordinate space. The transport optimization target for QOS is $dJ^*/d\theta = 0$ which is the omnigenity condition $J^* = J^*(\Phi)$. Progress²⁰ has been made in relating this omnigenity condition to $|B|$, and this may lead to additional physics targets. The degree of quasi-axisymmetry (or omnigenity) attained is assessed by using Monte Carlo methods and semi-analytical models to compute the confinement of thermal (and energetic) particles in a postoptimization analysis. The ISS95 empirical confinement scaling for the energy confinement time τ_E could be an additional transport target.

Typical stability targets are the Mercier criterion, resistive interchange (self-healing), high- n ballooning, and kink mode stability. Significant progress has been made integrating both ballooning and kink stability codes²¹ with the optimization process. For ballooning modes, coupling of fast matrix methods with variational techniques leads to ballooning eigenvalues which exhibit quartic mesh convergence. Richardson extrapolation then produces rapid convergence for the eigenvalue calculations on relatively coarse meshes. Appropriate centering of the outer conducting wall has made it possible to reliably and rapidly assess external kink stability for general three-dimensional boundaries.

Information about the complexity of the coils can also be added to χ^2 . One scheme being considered is based on minimizing the high- m Fourier modes of the surface current potential $\mu_0 |K| \equiv |B|$ at the plasma-vacuum interface. Another is to minimize curl K to reduce current vortices on the coil winding surface. In either case, these complexity measures are expected to provide feedback to the physics optimization regarding the realizability of the configuration.

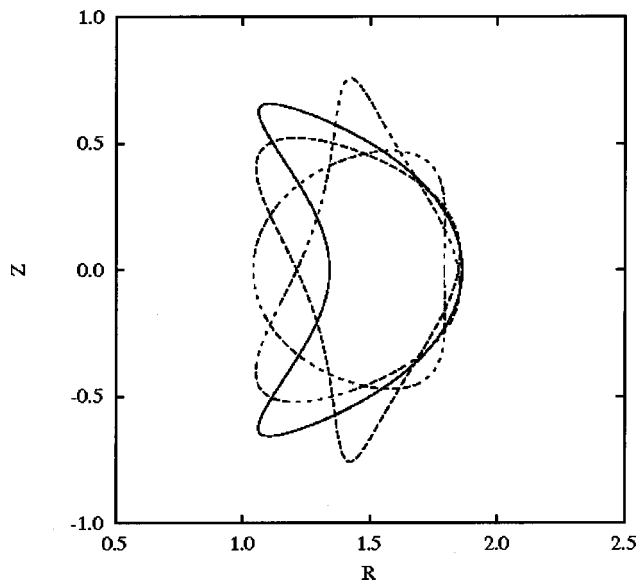


FIG. 2. Outer magnetic flux surfaces for the optimized PoP QAS described in the text, at toroidal cross sections $N\phi=0$ deg (solid), 45 deg and 135 deg (dashed), and 180 deg (dash-dot). Note the elongation and triangularity.

IV. COMPACT CONFIGURATIONS

In this section we describe the optimized compact stellarators under development. The NCSX is being proposed as a PoP device ($R \sim 1.5$ m, $B = 1 - 2$ T, $\langle \beta \rangle > 4\%$). The present QAS design²² achieves high β limits by using the ARIES-RS tokamak²³ boundary (with $\beta_{\text{balloon}} \approx 5\%$) as a fixed ($n=0$) part of the QAS boundary. This provides a strong component of ellipticity and triangularity to stabilize ballooning modes. QAS with $A=2.2$ has been found which has $\beta_{\text{balloon}} \approx 6\% - 7\%$, and configurations with stable betas $\approx 11\%$ have been obtained which also have reasonable quasi-symmetry and monotonic shear. For $A=3.4$, configurations with $\beta_{\text{balloon}} \approx 4\%$ have been found, consistent with the $1/A$ scaling expected for tokamaks.

The QAS design originated from an ARIES-RS tokamak equilibrium (with standard reverse-shear, ι decreasing at the edge) known to have good ballooning stability and transport. The ι profile was modified to produce the desired positive shear at the edge needed for island suppression and kink stability, while keeping the net parallel current nearly consistent with the bootstrap current. External seed currents can be reduced or eliminated in this way. Computationally, this is done by adding nonaxisymmetric ($n \neq 0$) components to the boundary in such a way as to maintain quasi-axisymmetry (thus ensuring good neoclassical transport), while fixing the $n=0$ shaping components (to retain high β_{balloon}). Depending on the helical components of the boundary, the amount of external transform is about 50% at the peak stable β . Figure 2 shows the outer surfaces at various toroidal angles for this resulting QAS. The strong shaping, needed for ballooning stability, is apparent.

To provide external kink stability on the timescales longer than the L/R time of the conducting wall, tokamaks will need to provide either multi-mode feedback stabilization or rapid rotation of the plasma (requiring recirculating

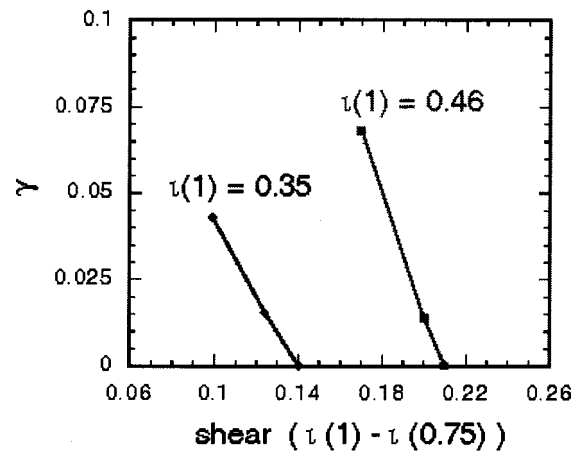


FIG. 3. External kink mode growth rate (γ) versus shear at the plasma edge for two different values of edge iota, $\iota(1)$, showing stabilization with increasing shear.

power). In QAS, the external kink mode can be stabilized both by imposing adequate externally generated shear and by a small amplitude, poloidally localized helical corrugation of the plasma boundary.^{6,7} Configurations which are stable to external kink modes at $\beta \approx 7.5\%$ have been found at wall separations equal to twice the minor radius (where they are thought to have little stabilizing influence). Figure 3 shows the stabilizing effect of increased edge shear on the kink mode growth rate for two different values of $\iota(1)$. As $\iota(1)$ increases, more shear is needed for stabilization. Figure 4 shows the stabilizing effect of a small externally imposed helical corrugation, which is localized on the outboard side of the plasma, for configurations with similar values of $\iota(1)$. The corrugation amplitude is small enough to maintain the

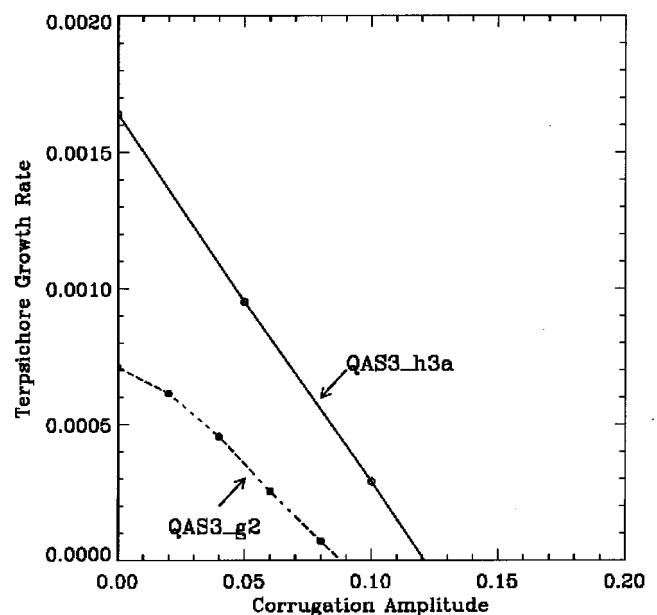


FIG. 4. External kink mode grown rate from the TERPSICHORE code versus corrugation amplitude produced by helical rippling of the plasma boundary. Complete kink mode suppression is possible, although the required boundary corrugation increases with the edge iota.

QA property of the equilibrium and could be produced by a set of Furth-Hartmann coils,²⁴ which are comprised of poloidally and toroidally localized windings typically located on the outboard side of the plasma.

QAS configurations with $A \approx 2.2$ have been examined with $N=2$ and $N=4$, which show excellent thermal confinement, having neoclassical ion confinement times only slightly below that in the equivalent tokamak. As mentioned before, the PBX-M geometry requires higher A (~ 3.4) plasma configurations. In these designs, the ripple portion of the neoclassical transport has been reduced below the axisymmetric part, but because of the larger A , and the modest ι (~ 0.4), the axisymmetric contribution to neoclassical transport in low-field ($B \sim 1T$) operation is limiting. Further physics optimization is needed to achieve a design of $\tau_E^{nc} \sim 3\tau_E^{ISS95}$ in order to realize energy confinement times $\tau_E = H\tau_E^{ISS95} = 21$ msec [for $T(0) = 1.3$ keV, $n(0) = 7 \times 10^{13}$ cm⁻³, $H=2$, $P=6$ MW] expected from the experimental stellarator data base.

Simulations of 40-keV neutral beam injection (NBI) have been performed for a PBX-M sized QAS. For the $N=2$, $A=2.2$ configuration (which had the lowest neoclassical transport of all configurations considered), it is found that all but parallel coinjection is unacceptable because of enhanced beam ion loss due to either pitch angle scattering into the ripple loss cone or prompt loss orbits. Alpha losses for a $R=4.5$ m, $B=7.9$ T reactor-sized QAS show a power loss of 8%. This may be acceptable, depending on the spatial deposition of the lost alphas.

Because of the small neoclassical parallel viscosity in a well-optimized QAS, flow-generated transport barriers and resulting H-mode energy confinement similar to tokamaks are expected. This is in contrast to conventional, unoptimized stellarators where toroidal rotation is strongly damped.

A QOS is being considered for a smaller, concept exploration (CE) experiment ($R \approx 1$ m, $B \approx 1$ T). QOS designs with stable ballooning and kink $\beta > 5\%$ have been previously studied. The available power for the CE experiments is about 4 MW radio frequency (RF), and this limits the attainable β ($\sim 2\%$). Because of the reliance on perpendicular heating in the CE phase, the CE QOS was designed to confine energetic ($E=20$ keV), deeply trapped particles, at the expense of β (although $\beta_{\text{balloon}} > 2\%$ was maintained).

The path to improved confinement at low A originated for the CE-sized QOS from a nearly quasi-helical state at $A=5$. Since the quasi-helical state is exactly omnigenous, it provided a good initial guess for the optimizer. As A was lowered toward $A \leq 3.6$, the quasi-helical symmetry was difficult to maintain, whereas the quasi-omnigenicity was more robust. For $N=3$, the iota profile was chosen as $0.66 < \iota < 0.74$ to avoid low order resonances, although $\iota(0) \geq 0.60$ is possible to increase the shear. These values of ι are sufficient to limit the ‘‘banana’’ widths of the energetic circulating orbits so they are well confined for $B=1T$. The magnetic surfaces for this configuration are shown in Fig. 5. The helical axis excursion is required to produce the specified ι from external coils. The $|B|$ spectrum for this device is a hybrid of a quasi-helical state (HSX-like), in which the m

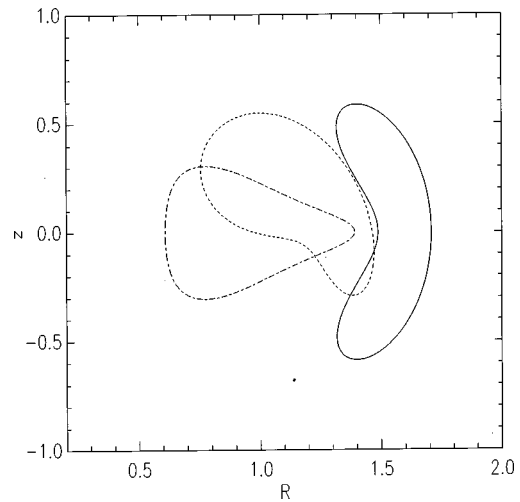


FIG. 5. Outer magnetic flux surfaces for the optimized CE QOS at toroidal cross sections $N\phi=0$ deg (solid), 45 deg (dashed), and 180 deg (dash-dot).

$=1$, $n=1$ mode dominates and the $1/R$ ($m=1$, $n=0$) component was suppressed (effective magnetic ‘‘aspect ratio’’ >10), and a W7X-like state consisting of a substantial ‘‘bumpy’’ field ($m=0$, $n=1$) with about half the amplitude at the edge of the helical component. The reduced bumpy field is a result of the increased magnetic aspect ratio (requiring less $1/R$ drift to be cancelled). For this configuration, the expected energy confinement time is $\tau_E = H\tau_E^{ISS95} \approx 11.4$ msec [$(n(0) = 5 \times 10^{13}$ cm⁻³, $P=2$ MW, $H=2$, yielding $T(0) \approx 1$ keV]. The neoclassical confinement time varies from 10 msec with no radial electric field to 25 msec for $e\phi/kT=2$.

A distinctive feature of QOS is the sensitive dependence²⁵ of the bootstrap current on the ratio B_{10}/B_{11} . By varying this ratio with external coil currents, the dependence of self-healing on the direction of j_{bs} (relative to the shear) can be studied in the CE device. Although calculations of j_{bs} for the CE QOS are presently underway, previous QOS configurations (with a larger ‘‘bumpy’’ field B_{10}) indicated reductions in j_{bs} by factors of at least 3 (compared to a tokamak) can be obtained. It is possible that reduced levels of j_{bs} in QOS may allow flatter ι -profiles (less shear), while maintaining external kink stability. However, lower j_{bs} also reduces the ‘‘self-healing’’ effect which, in QAS, gives access to larger shear at high β . One goal of a CE QOS experiment would be to explore the effect of j_{bs} (net current) on the kink and ballooning stability properties of such devices at moderate β .

V. COILS

The physics designs discussed in Sec. IV produce plasma boundaries from which coils can be calculated using NESCOIL.²⁶ In NESCOIL, the vanishing (in a least-squares sense) of the normal component of the magnetic field on the plasma surface determines a surface current potential K . A winding surface, usually at a fixed separation Δ from the plasma surface, is chosen *a priori*. For NCSX, existing toroidal and poloidal field coils are candidates to produce the main axisymmetric fields, and this raises the possibility of

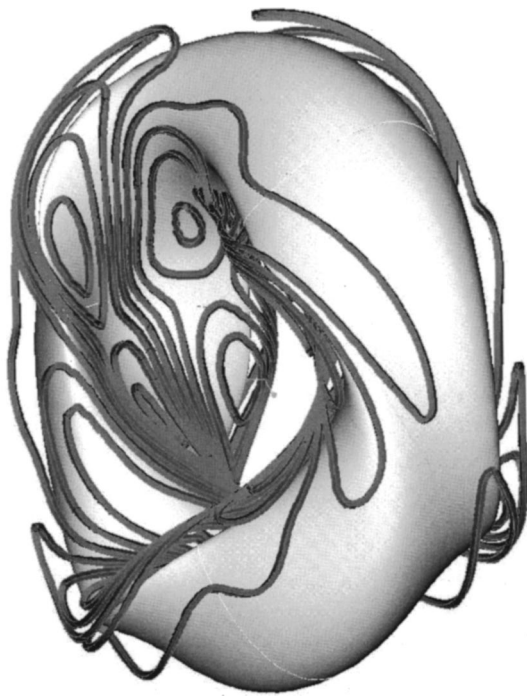


FIG. 6. Saddle coils for QAS with $N=3$ and $A=3.4$, enclosing the last flux surface.

using saddle coils to produce the remaining helical field. In contrast, the CE QOS has been designed solely with modular coils. (While modular coils encircle the plasma poloidally, thus producing both toroidal and helical fields, saddle coils do not encircle the plasma at all.)

For QAS, saddle surface current solutions with $A_{\Delta} < 7$ have been found with a normal field error on average $< 0.2\%$ (maximum error $< 2\%$). As A_{Δ} decreases (increased coil-plasma separation), it has been possible, by using singular value decomposition (SVD), to find smooth solutions for K with acceptable errors, even for $A_{\Delta} \approx 3$. The SVD technique allows the controlled removal of small (“singular,” physically irrelevant) eigenvalues from the ill-conditioned matrix equation²⁶ determining K .

The magnetic field produced by this current sheet solution has been used to reconstruct free-boundary magnetic surfaces and confirms that the desired physics properties were preserved. As the sheet current is discretized into a finite number of coils, the field errors remain nearly unchanged, but the reconstructed surfaces computed from these discrete coils depart significantly from the physics target when the number of coils is too few. A preliminary set of saddle coils for the $N=3$, $A=3.4$ QAS is shown in Fig. 6, with $N_c=8$ coils per period.

This reconstruction error is thought to result from resonant components of the normal field errors introduced by the discretization of K . In vacuum, field-line tracing shows that magnetic islands and a stochastic edge correlate with poor reconstructability. Further investigation at finite β is underway by modifying NESCOIL to compute the displacement w at the outer boundary, where $B_0 \cdot \nabla w = \delta B^{\psi}$. Here δB^{ψ} is the normal component of the magnetic field error, and B_0 is the unperturbed magnetic field. The possibility of using error

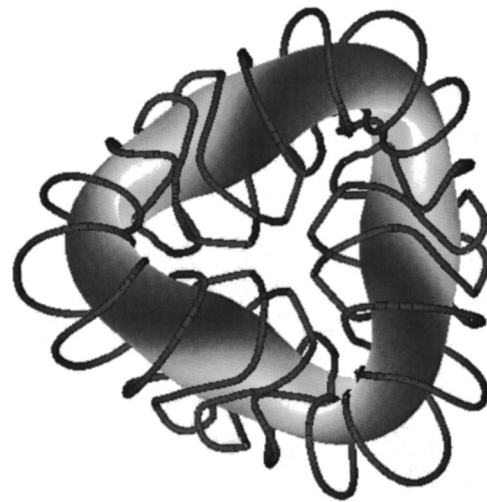


FIG. 7. Modular coils for QOS with $N=3$ and $A=3.5$, enclosing the last flux surface.

correction coils to cancel resonant components of δB^{ψ} is also under consideration.

For QOS, a set of modular coils has been designed for the CE experiment. Values of $A_{\Delta} < 7$ have been achieved, but lower values will be sought using SVD methods. A QOS coil set for $N=3$, $N_c=7$ modular coils per period, is shown in Fig. 7. The average normal field error for these coils is an order of magnitude larger (3%) than for the QAS configuration. Nevertheless, the physics properties are preserved by the reconstructed surfaces, indicating that the resonant error was suppressed for these modular coils.

For compact stellarators, the low values of A imply tight packing of coils, especially on the inboard side. The increased forces which result will have to be assessed, and appropriate support structures devised.

VI. DESIGN STATUS AND SUMMARY

The design of two compact stellarator configurations has been described. Access to low A has been achieved by relaxing the prohibition on net current found in larger A stellarators. The QAS is a stellarator with many features in common with tokamaks, including sizeable bootstrap current at finite β and high ballooning β limits. In contrast to tokamaks, however, QAS will have external transform to reduce the need for externally driven seed currents, and the possibility of monotonically increasing iota profiles and helical boundary corrugations to provide steady-state kink stability. Although disruption suppression has been observed even with modest amounts of external transform in ohmic current discharges in W7-A, experimental studies will be needed to determine under what conditions bootstrap currents may reintroduce a free energy source to drive disruptions in QAS. Also, it will be necessary to develop start-up scenarios that do not depend on ohmic current, although inductive current drive will be provided for experimental flexibility. The QAS represents an evolutionary path for toroidal confinement systems which makes use of nonsymmetric shaping and external transform to provide additional stability control without sac-

rificing good confinement properties. The final QAS will combine the favorable attributes of positive edge shear with an adequate degree of neoclassical confinement into a single, unified, and constructable design. Present QAS designs have already achieved gap ratios $A_{\Delta} < 7$ (and even $A_{\Delta} \approx 3$) with promising implications for reactor scalability.

The QOS has at least two different helical components in its $|B|$ spectrum. This feature gives QOS the ability to run with a smaller contribution to the total transform arising from bootstrap currents, thus making its magnetic configuration somewhat invariant to variations in β (similar to W7-X). Because of the smaller fraction of internally generated transform and the helical bumpiness of $|B|$, relatively low values of N ($N \leq 4$) are needed to achieve small values of A_{Δ} . The presently achieved values of $A_{\Delta} \sim 7$ must be lowered before QOS will extrapolate to a compact reactor. The small bootstrap current, inherent to the CE-sized QOS, reduces the free energy available for kinks and vertical displacements, but also leads to lower ballooning limits than found in QAS. A challenge facing the QOS design will be to raise the ballooning β while maintaining the good confinement properties of the CE design.

ACKNOWLEDGMENTS

This research was sponsored by the Office of Fusion Energy Sciences, U.S. Department of Energy, under Contract No. DE-AC0596OR22464 with Lockheed Martin Energy Research Corporation. The authors would like to thank M. Drevlak and P. Merkel for making available the NESCOIL code; W. A. Cooper for providing the TERPSICHORE code; C. Nührenberg for help with kink-mode calculations; P. Moroz and M. Hughes for performing bootstrap current calculations; and A. S. Ware for improvements to the stellarator optimization code.

¹K. Matsuoka, S. Kubo, M. Hosokawa *et al.*, Plasma Physics and Controlled Nuclear Fusion Research, Proceedings 12th International Conference, Nice, 1988 (International Atomic Energy Agency, Vienna, 1989), Vol. 2, p. 411.

²R. F. Gandy, M. A. Henderson, J. D. Hanson *et al.*, Fusion Technol. **18**, 281 (1990).

³G. Grieger, C. D. Beidler, H. Maassberg *et al.*, Plasma Physics and Controlled Nuclear Fusion Research, Proceedings 13th International Confer-

ence, Washington, 1990, Vol. 3, p. 525 (International Atomic Energy Agency, Vienna, 1991).

⁴D. T. Anderson, Proc. J. Plasma Fusion Res. SERIES, Vol. 1 (1998).

⁵J. N. Nührenberg, W. Lotz, and S. Gori, *Theory of Fusion Plasma*, Varenna, 1994 (Editrice Compositori, Bologna, 1994); P. Garabedian, Phys. Plasmas **3**, 2483 (1996).

⁶S. Gori, W. Lotz, J. Nührenberg, *Theory of Fusion Plasmas*, edited by J. W. Connor *et al.* (Editrice Compositori, Bologna, 1996), p. 335; S. P. Hirshman *et al.*, Phys. Rev. Lett. **80**, 528 (1998).

⁷G. Fu, private communication. This is similar to stabilization of high mode number internal modes in tokamaks. See J. Wesson, Nucl. Fusion (1978).

⁸B. Blackwell and N. Pomphrey, private communication, see H. P. Furth and C. W. Hartman, Phys. Fluids **11**, 408 (1968).

⁹D. Anderson, D. Batchelor, A. Boozer *et al.*, "Stellarator Proof of Principle Program," May 1998, private communication.

¹⁰U. Stroth, M. Murakami, R. A. Dory *et al.*, Nucl. Fusion **36**, 1063 (1996).

¹¹B. A. Carreras, N. Dominguez, L. Garcia *et al.*, Nucl. Fusion **28**, 1195 (1988).

¹²W VII-A Team, Nucl. Fusion **20**, 1093 (1980).

¹³J. R. Cary and M. Kotschenreuther, Phys. Fluids **28**, 1392 (1985); C. C. Hegna and A. Bhattacharjee, Phys. Fluids B **1**, 392 (1989).

¹⁴R. Goldston, in Innovative Confinement Concepts Workshop 1997, Santa Monica, CA, March 3–6, 1997.

¹⁵J. Nührenberg, W. Lotz, P. Merkel *et al.*, Trans. Fusion Technol. **27**, 71 (1995).

¹⁶D. A. Spong, S. P. Hirshman, J. C. Whitson *et al.*, Phys. Plasmas **5**, 1752 (1998).

¹⁷S. P. Hirshman, W. I. van Rij, and P. Merkel, Comput. Phys. Commun. **43**, 143 (1986).

¹⁸K. C. Shaing, E. C. Crume, J. S. Tolliver *et al.*, Phys. Fluids B **1**, 148 (1989); K. Watanabe, T. Sato, and Y. Nakayama, Nucl. Fusion **35**, 335 (1995).

¹⁹R. B. White, D. Monticello, Z. Lin, and S. P. Hirshman, submitted to Phys. Plasmas.

²⁰J. R. Cary and S. G. Shasharina, Phys. Rev. Lett. **78**, 674 (1997); A. A. Skovoroda and V. D. Shafranov, Phys. Plasmas Rep. **21**, 937 (1995); H. Weitzner, Phys. Plasmas **4**, 575 (1997); S. Gori *et al.*, in Proceedings Varenna-Lausanne International Workshop on Theory of Fusion Plasmas, edited by J. W. Connor, *et al.* (Editrice Compositori, Bologna, 1997).

²¹W. A. Cooper, D. B. Singleton, and R. L. Dewar, Phys. Plasmas **3**, 275 (1996); C. Schwab, Phys. Fluids B **5**, 3195 (1993); R. Sanchez *et al.*, Nucl. Fusion **37**, 1363 (1997).

²²A. Reiman, L. Ku, D. Monticello *et al.*, "Physics Issues in the Design of a High β Quasi-Axisymmetric Stellarator," Yokohama, 1998 (International Atomic Energy Agency, Vienna).

²³S. C. Jardin, C. E. Kessel, C. G. Bathke *et al.*, Fusion Eng. Des. **38**, 27 (1997).

²⁴H. P. Furth and C. W. Hartman, Phys. Fluids **11**, 408 (1968).

²⁵H. Maassberg, W. Lotz, J. Nührenberg *et al.*, Phys. Fluids B **5**, 3728 (1993).

²⁶P. Merkel, Nucl. Fusion **27**, 867 (1987).